Available online at www.sciencedirect.com

SciVerse ScienceDirect

Ceramics International 39 (2013) 3865–3871

CERAMICS INTERNATIONAL

www.elsevier.com/locate/ceramint

Effect of $PbTiO_3$ seed layer on the orientation behavior and electrical properties of $Bi(Mg_{1/2}Ti_{1/2})O_3$–$PbTiO_3$ ferroelectric thin films

Longdong Liu[a], Ruzhong Zuo[a,*], Qi Liang[b]

[a]*Institute of Electro Ceramics and Devices, School of Materials Science and Engineering, Hefei University of Technology, Hefei 230009, PR China*
[b]*Center for Nanomaterial and Nanodevice, School of Physical Science, Hefei University of Technology, Hefei 230009, PR China*

Received 25 September 2012; received in revised form 19 October 2012; accepted 19 October 2012
Available online 26 October 2012

Abstract

High Curie-temperature $0.63Bi(Mg_{1/2}Ti_{1/2})O_3$–$0.37PbTiO_3$ (BMT–PT) films were fabricated on $Pt(111)/Ti/SiO_2/Si$ substrates by the sol–gel spin-coating method. The oriented growth behavior of thin films was controlled by introducing a PT seed layer onto the platinum electrode surface. The effect of the annealing method of the PT seed layer on the orientation behavior and electrical properties of BMT–PT films was investigated. It was found that BMT–PT thin film exhibits higher (100) orientation degree when the PT seed layer was treated by rapid thermal annealing. The dielectric permittivity increases while the remanent polarization and coercive field decrease with increasing the (100) orientation degree. These results were explained according to the relationship between the preferential orientation and the spontaneous polarization directions of the films.

Keywords: A. Films; C. Electrical properties; D. Perovskites; Sol–gel processes

1. Introduction

Much attention has been paid to the ferroelectric thin films with high Curie temperatures because both high electrical performances and good temperature stability are required for applications in automotive, aerospace, and related industries [1–3]. As one of the potential candidates, the $BiMeO_3$–$PbTiO_3$ solid solution system has been studied in the form of ceramics or films, such as $BiScO_3$–$PbTiO_3$ (BS–PT) [4], $Bi(Ni_{1/2}Ti_{1/2})O_3$–$PbTiO_3$ (BNT–PT) [5], and $Bi(Mg_{1/2}Ti_{1/2})O_3$–$PbTiO_3$ (BMT–PT) [6]. BS–PT thin films prepared by pulse laser deposition (PLD) or the sol–gel method were reported to exhibit good electrical properties [1,2,7]. BNT–PT thin films prepared by PLD have also been investigated in recent years [8]. However, the potential applications of BS–PT and BNT–PT systems could be limited by the high cost of scandium sources and the relatively high dielectric loss, respectively. By comparison, BMT–PT compositions might own some advantages from the application point of view. The sol–gel derived 0.63BMT–0.37PT thin films close to the morphotropic phase boundary (MPB) were reported to exhibit good dielectric and ferroelectric properties [9].

It was known that the properties of ferroelectric films are dependent on a few parameters, including composition [10], grain size [11], orientation [2,10,12], and film thickness [13], etc. Previous studies have demonstrated that highly oriented ferroelectric thin films could exhibit significantly enhanced properties [2,10]. However, the orientation of the deposited films is closely correlated with processing parameters such as the precursor preparation [14], pyrolysis temperature [15], annealing temperature [16], heating rate [17], appropriate substrates [18], textured conductive oxide electrodes [19], seed layer [20–23], and so on. Recent studies showed that seed layer is more effective in growing the textured films. Fu et al. deposited PbO on the substrate as a seed layer to control the texture of lead zirconate titanate (PZT) thin films [20]. Muralt et al. reported that (111) textured PZT films can be obtained using TiO_2 seed layer [21]. And some others deposited PT seed layer to obtain oriented PZT thin films. Zeng et al. obtained (100) oriented PZT thin films when the PT seed layer was baked at 300 °C for 30 min and crystallized at 600 °C for 90 min

*Corresponding author. Tel./fax: +86 551 2905285.
E-mail address: piezolab@hfut.edu.cn (R. Zuo).

0272-8842/$ - see front matter © 2012 Elsevier Ltd and Techna Group S.r.l. All rights reserved.
http://dx.doi.org/10.1016/j.ceramint.2012.10.229

[22]. Kim et al. demonstrated that when the PT seed layers were dried at 300 °C for 5 min, and then annealed at 650 °C for 1 min using rapid thermal annealing (RTA), the PZT thin films exhibited (111) orientation [23]. The seed layer seems effective in growing the textured films, but it can be seen that different annealing methods of the seed layer would result in various orientation behavior.

In this work, a conventional sol–gel process and spin-coating method were applied to make BMT–PT ferroelectric thin films. The oriented growth of the as-deposited BMT–PT films was induced by a PT seed layer, which was first deposited on $Pt/Ti/SiO_2/Si$ substrates before the BMT–PT films were coated. The effect of the annealing method of the seed layer on the orientation behavior and electrical properties of BMT–PT thin films was investigated in detail.

2. Experimental

BMT–PT precursor solution with an MPB composition (37 mol% PT, 10 mol% Pb and Bi excess) was prepared by the sol–gel method as described elsewhere [9]. Precursor solution of the PT seed layer was synthesized via a similar process to the BMT–PT precursor solution. Firstly, trihydrated lead acetate $[Pb(OOCCH_3)_2 \cdot 3H_2O]$ was dissolved in glacial acetic acid and Tetrabutyl titanate $[Ti(OC_4H_9)_4]$ was dissolved in 2-methoxyethanol (2-MOE) with acetylacetone as the stabilizer and chelating agents, respectively. Then, the $Ti(OC_4H_9)_4$ solution was added to the $Pb(OOCCH_3)_2$ solution and stirred 24 h to form PT precursor solution with a concentration of 0.05 M.

The PT seed layer was prepared onto $Pt/Ti/SiO_2/Si$ substrates by a spin-coating process at 4000 rpm for 30 s. After drying at 200 °C for 5 min, the PT seed layer was either annealed at 650 °C for 5 min using a typical RTA process, i.e., directly putting the sample into the furnace at 650 °C, or annealed at 650 °C for 30 min by a conventional thermal annealing (CTA) process with a heating rate of 10 °C/min. Afterwards, the BMT–PT thin films were deposited onto the PT layer-coated substrates by a repeated spin-coating process at 4000 rpm for 30 s. For comparison, the thin film sample without PT seed layers was also prepared. After each spin-coating step, the BMT–PT films were dried at 200 °C for 5 min, and pyrolyzed at 500 °C for 8 min under ambient atmosphere. Finally, the as deposited films were annealed at 675 °C for 30 min by CTA. For electrical measurement, top Ag electrodes of 0.2 mm diameter were deposited through a shadow mask by means of a thermal evaporation method.

The phase structures were characterized by an X-ray diffractometer (XRD, D/MAX2500V, Rigaku, Japan) with Cu Kα radiation. The surface microstructure of the BMT–PT thin films was observed by an atomic force microscope (AFM, Being Nano-Instruments CSPM-4000, Beijing, China). The microstructure on the surface and fractured cross-section of BMT–PT thin films without PT seed layer was observed by a field-emission scanning electron microscope (FE-SEM, Sirion200, FEI, Hillsboro, OR). The dielectric properties (permittivity and loss tangent) as a function of frequency were measured by a precision impedance analyzer (HP 4194A, Hewlett-Packard, Palo Alto, CA). A ferroelectric testing system (Precision LC, Radiant Technologies Inc., Albuquerque, NM) was used to evaluate the ferroelectric properties of the films.

3. Results and discussion

Fig. 1 shows the XRD patterns of the BMT–PT films deposited on $Pt/Ti/SiO_2/Si$ substrates and PT seed layer coated $Pt/Ti/SiO_2/Si$ substrates, respectively. It can be seen that all films exhibit a pure perovskite structure. The [100] peak shows a slight splitting and the [110] diffraction peak is obviously split into [101] and [110] lines, suggesting that the film composition should be in the tetragonal-rich side of the MPB. The introduction of the PT seed layer has an obvious effect on the orientation of the thin films. The BMT–PT films with PT seed layer are preferentially (100) oriented, regardless of the annealing methods of the seed layer. However, as the seed layer was treated by RTA, the BMT–PT thin film shows a much higher orientation degree. A Lotgering factor [24] was used to describe the degree of (100) orientation, which was 0.5, 0.65, and 0.76 for the BMT–PT thin films without seed layer, and with PT seed layer annealed by CTA and RTA, respectively.

To investigate the reason for the orientation behavior, the XRD patterns of the PT seed layer are shown in Fig. 2. It can be found that all PT seed layers show (100) preferential orientation although they were annealed by different methods. The PT seed layer annealed by RTA exhibits a much higher degree of (100) orientation. The PT seed layer can provide energetically favorable nucleation sites and decrease the nucleation energy, promoting the formation of similarly oriented crystallites to the PT seed

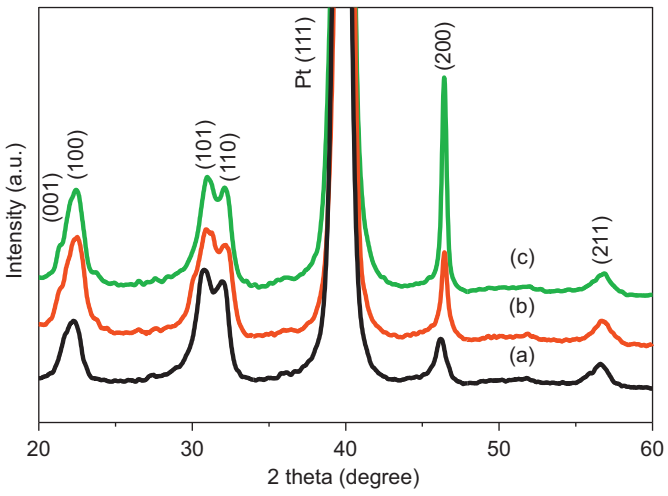

Fig. 1. XRD patterns of BMT–PT thin films: (a) without seed layer, (b) with PT seed layer annealed at 650 °C for 30 min by CTA, and (c) with PT seed layer annealed at 650 °C for 5 min by RTA.

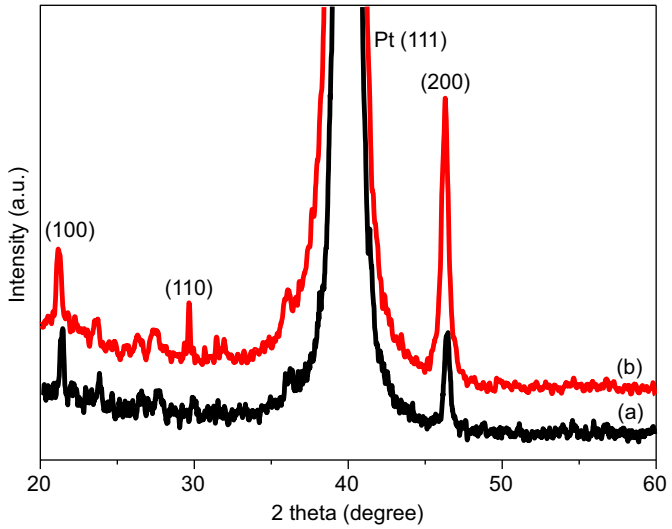

Fig. 2. XRD patterns of the PT seed layer: (a) annealed at 650 °C for 30 min by CTA, and (b) annealed at 650 °C for 5 min by RTA.

layer in the BMT–PT thin films. As a result, the BMT–PT films develop similar crystallographic orientation to the PT seed layer. The formation of (100) oriented PT seed layer is probably due to an inherent self-orientation tendency in which the plane has the lowest surface energy. In the case of the perovskite structure of PT phase, the (100) plane is considered to have the lowest surface energy [25]. While the difference in the orientation degree caused by different annealing methods might be because RTA produces a directional heat flow, leading to a temperature gradient across the film-substrate interface and promoting the nucleation at this interface [26]. The surface morphology of the PT seed layer is shown in Fig. 3. It can be seen the seed layers look discontinuous, probably owing to the limited concentration of the precursor solution. These discontinuous islands can act as the nucleation sites, such that the film of the PT seed layer can be formed.

Fig. 4 displays the surface morphology of the BMT–PT thin films without seed layer and with PT seed layers annealed by different methods. It can be seen that the BMT–PT thin films with seed layer exhibit much denser and more smooth surface and smaller grain size. The surface roughness of the films were 3.4 nm, 2.7 nm, and 2.9 nm for the BMT–PT film without seed layer, with PT seed layer annealed by CTA and RTA, respectively. The reduction of the grain size for the film with PT seed layer would be related to the PT seed layer provides nucleation sites for BMT–PT thin films, which could promote the crystallization of BMT–PT thin films and change the crystallization mechanism from homogeneous nucleation to heterogeneous nucleation. Generally, heterogeneous nucleation could promote the nucleate rate while inhibit the grain growth, so that the grain size is reduced and the film surface becomes more smooth. The microstructure on the surface and fractured cross-section of the film without PT seed layer is shown in Fig. 5. It can be seen that the developed BMT–PT film has a relatively dense structure.

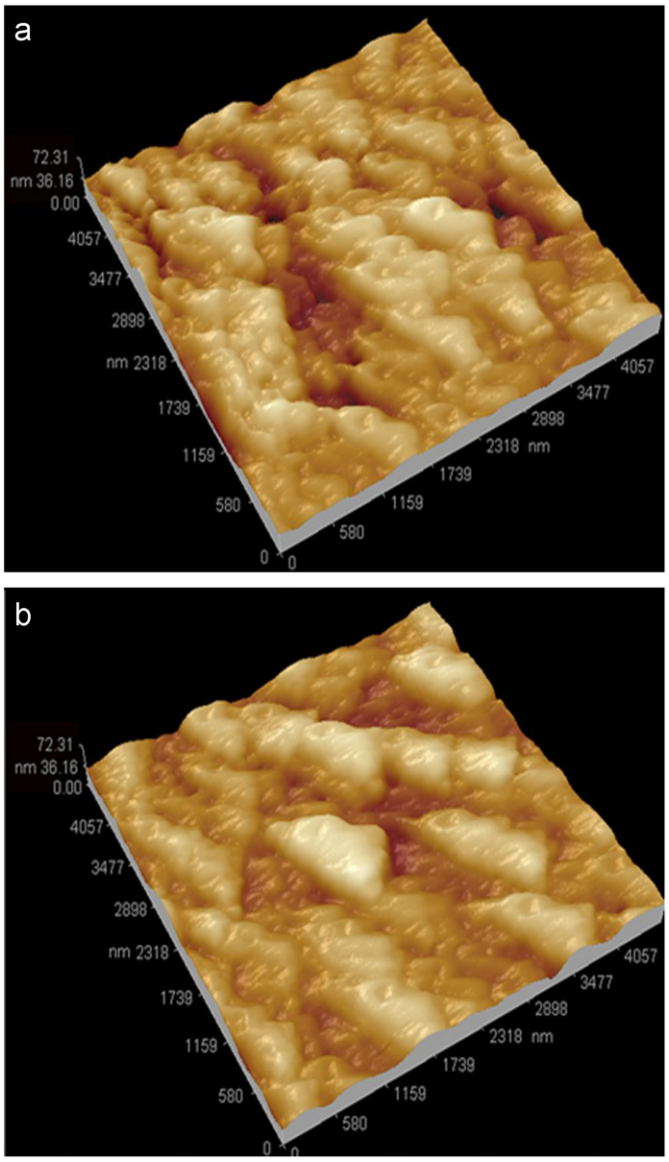

Fig. 3. Surface morphology of the PT seed layer: (a) annealed at 650 °C for 30 min by CTA, and (b) annealed at 650 °C for 5 min by RTA.

The cross-sectional graph shows that the film has an estimated thickness of 375 nm, and sticks well to the substrate. No distinct interfaces could be observed between deposited layers formed after each spin-coating step.

Frequency dependence of the dielectric permittivity and dissipation factor for the BMT–PT thin films with and without PT seed layer is shown in Fig. 6. Apparently, the BMT–PT thin films with PT seed layer show larger dielectric permittivity and lower loss tangent value as compared to those without PT seed layer. Furthermore, it can be seen that the dielectric permittivity of the film with the PT seed layer annealed by RTA is much larger than that of the film with the PT seed layer annealed by CTA. This result might be related to the degree of (100) orientation. The reason why the (100) oriented film demonstrates larger dielectric permittivity was given as

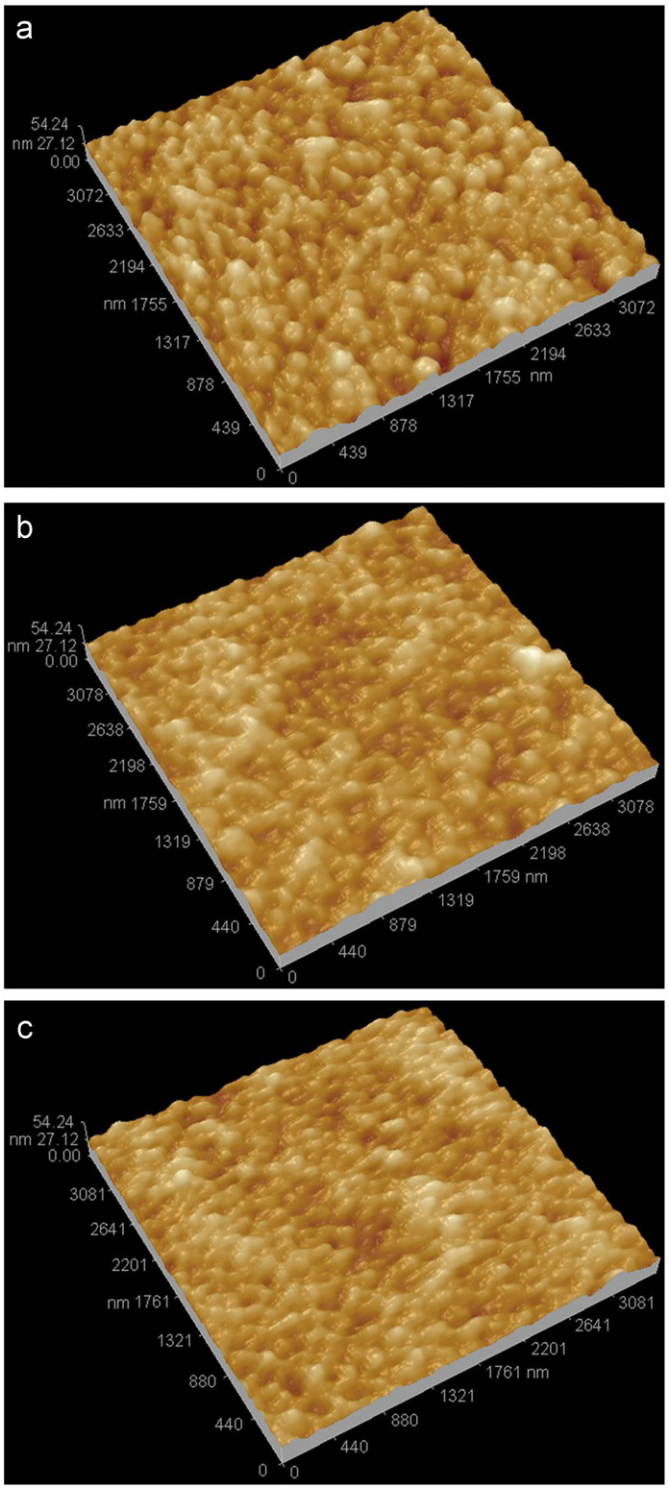

Fig. 4. AFM morphology of the BMT–PT thin films: (a) without seed layer, (b) with PT seed layer annealed at 650 °C for 30 min by CTA, and (c) with PT seed layer annealed at 650 °C for 5 min by RTA.

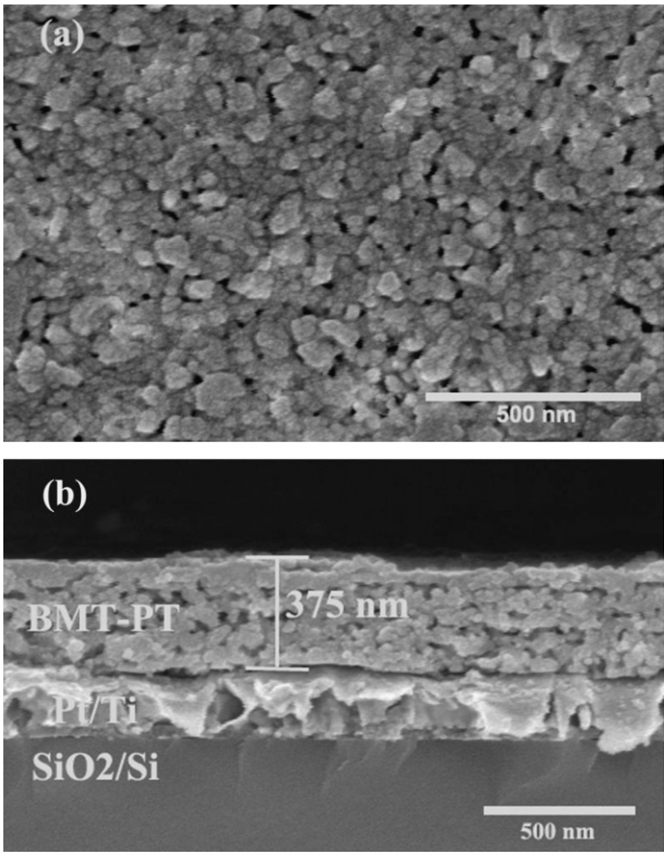

Fig. 5. SEM images on the surface (a) and cross section (b) of the BMT–PT thin films without seed layer observed by SEM.

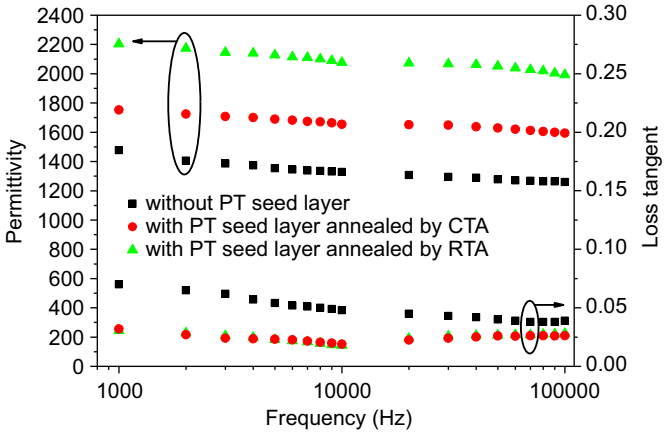

Fig. 6. Dielectric permittivity and loss tangent as a function of frequency for the various BMT–PT thin films as indicated.

follows: Du et al. have reported theoretical calculations based on the phenomenological consideration of the crystal orientation dependence of the dielectric and piezoelectric properties. For both tetragonal and rhombohedral phases, the dielectric permittivity monotonously increases as the crystal cutting angle from the spontaneous polarization direction increases, and the maximum value of dielectric permittivity is in the direction perpendicular to the spontaneous polarization direction [27]. The possible orientation of the polarization vector for the (100) oriented tetragonal perovskite film is schematically shown in Fig. 7(a). The dipole vibration prefers to follow the four-fold axis of the oxygen octahedron, which is in the [001] direction [28]. The (100) oriented tetragonal thin films should exhibit the maximum dielectric permittivity,

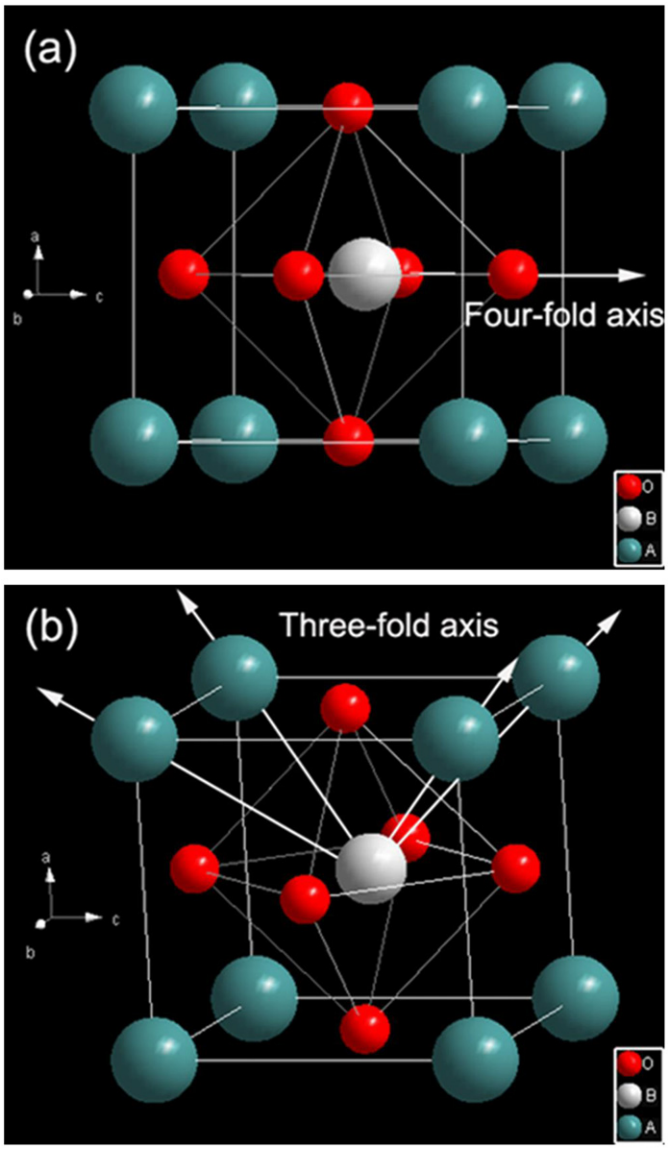

Fig. 7. Schematic illustration of the possible polarization vectors in the (100) oriented (a) tetragonal and (b) rhombohedral films.

because their preferential orientation is perpendicular to the spontaneous polarization direction. In the case of a rhombohedral perovskite, the spontaneous polarization orientation follows the three-fold axes of the oxygen octahedron, which is in the [111] direction [29]. The spontaneous polarization orientation cants an angle of about 54.7° to the normal of the film, as shown in Fig.7(b). The polarization direction of the (100) oriented rhombohedral film is titled away from the normal to the film surface. As a result, the increase of the (100) orientation degree tends to enhance the dielectric permittivity [29,30]. Moreover, the loss tangent value of the BMT–PT thin films with PT seed layer were apparently reduced, properly because they are denser than those without the PT seed layer. Usually, the moisture is easily adsorbed on the surface of the open pore channels, which would result in an increase of the dielectric loss [31].

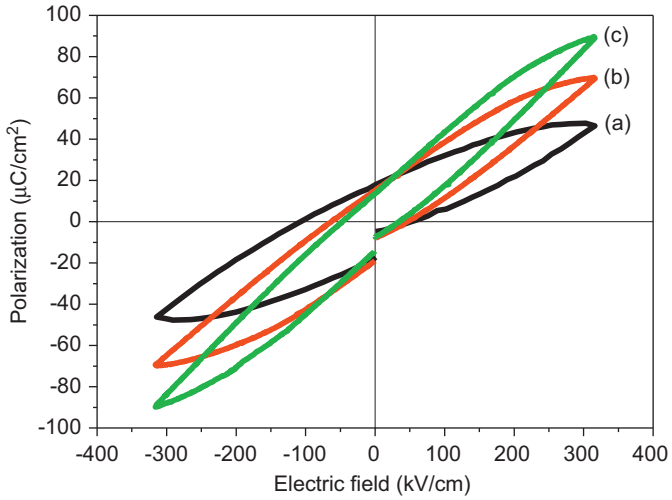

Fig. 8. *P–E* hysteresis loops of the BMT–PT thin films: (a) without seed layer, (b) with PT seed layer annealed at 650 °C for 30 min by CTA, and (c) with PT seed layer annealed at 650 °C for 5 min by RTA.

Fig. 8 shows the polarization versus electric field (*P–E*) hysteresis loops of the BMT–PT films with and without PT seed layer measured at 1 kHz. It can be seen that the shape of the hysteresis loop of the film was not saturated owing to the leakage current. Higher conductivity of BMT–PT materials has been reported even for bulk ceramics [32,33]. This can be modified by adding a few dopants such as Mn^{2+}. The relevant work has been reported elsewhere [34]. The remanent polarization (P_r) are 17.8, 15.1, and 13.8 μC/cm^2, and the coercive field (E_c) are 52.3, 43.7, 34.9 kV/cm for the BMT–PT film without seed layer, with PT seed layers annealed by CTA and RTA, respectively. It can be seen that the (100) textured BMT–PT films show lower P_r and lower E_c values. As known, the [100] direction is not the possible polarization orientation in both tetragonal and rhombohedral phases. For a tetragonal phase, the spontaneous polarization orientation is in the [001] direction, whereas for a rhombohedral phase, it is in the [111] orientation [28]. Therefore, the P_r value decreases with increasing the (100) orientation degree of the film. Another possible reason can be ascribed to the smaller grain size for the BMT–PT thin films with PT seed layer (see Fig. 4). The effect of grain size on the ferroelectric properties has been discussed previously [9]. Moreover, because the tetragonal phase usually has a spontaneous polarization orientation along [001] direction, parallel to the film surface, it mainly consists of in-plane domains that are hard to reorient and could contribute to the polarization only under a large electric field [30]. The obtained polarization then mainly results from the out-of-plane domain switching, which is relatively easy and would not induce the internal field stress. For a rhombohedral phase, all polarization directions cant the same angle of about 54.7° to the normal of the film surface and contribute equally to the measured polarization value. The switching of these kinds of domains does not change the dimension of the (100) oriented film along the direction

normal to the film surface [28], and would not induce strains. Thus, the back-switching of the domains is much easier for the film with higher (100) orientation degree. As a result, the P_r and E_c values of the BMT–PT films are reduced as the (100) orientation degree increases.

4. Conclusions

The 0.63BMT–0.37PT MPB films were successfully prepared on Pt/Ti/SiO_2/Si substrates and PT seed layer coated Pt/Ti/SiO_2/Si substrates by means of a conventional sol–gel spin-coating method. The introduction of the PT seed layer would help promote the formation of (100) preferentially oriented BMT–PT films, which is, however, dependent on the annealing method of the seed layer. The BMT–PT thin film with the PT seed layer annealed by RTA exhibits a higher (100) orientation degree. The more highly (100) textured BMT–PT thin films show larger dielectric permittivity, smaller loss tangent, and smaller P_r and E_c values.

Acknowledgments

This work was financially supported by a project of Natural Science Foundation of Anhui province (1108085J14) and the National Natural Science Foundation of China (50972035 and 51272060).

References

[1] T. Yoshimura, S.T. Mckinstry, Growth and properties of (001) $BiScO_3$–$PbTiO_3$ epitaxial films, Applied Physics Letters 81 (2002) 2065–2066.

[2] H. Wen, X.H. Wang, C.F. Zhong, L.K. Shu, L.T. Li, Epitaxial growth of sol–gel derived $BiScO_3$–$PbTiO_3$ thin film on Nb-doped $SrTiO_3$ single crystal substrate, Applied Physics Letters 90 (2007) 202902-1–202902-3.

[3] M.A. Khan, T.P. Comyn, A.J. Bell, Large remanent polarization in ferroelectric $BiFeO_3$–$PbTiO_3$ thin films on Pt/Si substrates, Applied Physics Letters 91 (2007) 032901-1–032901-3.

[4] R.E. Eitel, C.A. Randall, T.R. Shrout, S.E. Park, Preparation and characterization of high temperature perovskite ferroelectrics in the solid solution $(1-x)BiScO_3$–$xPbTiO_3$, Japanese Journal of Applied Physics 41 (2002) 2099–2104.

[5] S.M. Choi, C.J. Stringer, T.R. Shrout, C.A. Randall, Structure and property investigation of a Bi-Based perovskite solid solution: $(1-x)$Bi(Ni1/2Ti1/2)O_3–$xPbTiO_3$, Journal of Applied Physics 98 (2005) 034108-1–034108-4.

[6] C.A. Randall, R. Eitel, B. Jones, T.R. Shrout, Investigation of a high T_c piezoelectric system: $(1-x)Bi(Mg_{1/2}Ti_{1/2})O_3$–$xPbTiO_3$, Journal of Applied Physics 95 (2004) 3633–3638.

[7] H. Wen, X.H. Wang, L.T. Li, Fabrication and properties of sol–gel-derived $BiScO_3$–$PbTiO_3$ thin films, Journal of the American Ceramic Society 89 (2006) 2345–2347.

[8] G.H. Wu, H. Zhou, N. Qin, D.H. Bao, Growth and electrical properties of 25%$Bi(Ni_{1/2}Ti_{1/2})O_3$–75%$PbTiO_3$ thin films on Pt/TiO_2/SiO_2/Si substrates using the pulsed laser deposition method, Journal of the American Ceramic Society 94 (2011) 1675–1678.

[9] L.D. Liu, R.Z. Zuo, Fabrication and electrical properties of sol–gel-derived 0.63$Bi(Mg_{1/2}Ti_{1/2})O_3$–0.37$PbTiO_3$ thin films, Journal of the American Ceramic Society 94 (2011) 3686–3689.

[10] T. Oikawa, M. Aratani, H. Funakubo, K. Saito, M. Mizuhira, Composition and orientation dependence of electrical properties of epitaxial $Pb(Zr_xTi_{1-x})O_3$ thin films grown using metalorganic chemical vapor deposition, Journal of Applied Physics 95 (2004) 3111–3115.

[11] S.B. Ren, C.J. Lu, J.S. Liu, H.M. Shen, Y.N. Wang, Size-related ferroelectric-domain-structure transition in a polycrystalline $PbTiO_3$ thin film, Physical Review B 54 (1996) 14337–14340.

[12] W. Gong, J.F. Li, X.C. Chu, Z.L. Gui, L.T. Li, Single-crystal Nb-doped Pb(Zr, Ti)O_3 thin films on Nb-doped $SrTiO_3$ wafers with different orientations, Applied Physics Letters 85 (2005) 3818–3820.

[13] Y. Sakashita, H. Segawa, K. Tominaga, M. Okada, Dependence of electrical properties on film thickness in $Pb(Zr_xTi_{1-x})O_3$ thin films produced by metalorganic chemical vapor deposition, Journal of Applied Physics 73 (1993) 7857–7863.

[14] C.K. Kwok., S.B. Desu, D.P. Vijay, Modified sol–gel process for preparation of lead zirconate titanate thin films, Ferroelectrics Letters Section 16 (1993) 143–156.

[15] W. Gong, J.F. Li, X.C. Chu, L.T. Li, Effect of pyrolysis temperature on preferential orientation and electrical properties of sol–gel derived lead zirconate titanate films, Journal of European Ceramic Society 24 (2004) 2977–2982.

[16] X.S. Li, T. Tanaka, Y. Suzuki, Preferred orientation and ferroelectric properties of lead zirconate titanate thin films, Thin Solid Films 375 (2000) 91–94.

[17] J. Lu, Y. Zhang, T. Ikehara, T. Mihara, R. Maeda, Effects of rapid thermal annealing on nucleation, growth, and properties of lead zirconate titanate films, IEEE Transactions on Ultrasonics, Ferroelectrics and Frequency Control 54 (2007) 83–86.

[18] D. Xie, T.L. Ren, L.T. Liu, The effect of substrate materials on orientation degree of lanthanum-substituted bismuth titanate thin films, Integrated Ferroelectrics 65 (2004) 3–11.

[19] M. Jain, B.S. Kang, Q.X. Jia, Effect of conductive $LaNiO_3$ electrode on the structural and ferroelectric properties of $Bi_{3.25}La_{0.75}Ti_3O_{12}$ films, Applied Physics Letters 89 (2006) 242903-1–242903-3.

[20] D.S. Fu, H. Suzuki, T. Ogawa, K. Ishikawa, High-piezoelectric behavior of *c*-axis-oriented lead zirconate titanate thin films with composition near the morphotropic phase boundary, Applied Physics Letters 80 (2002) 3572–3574.

[21] P. Muralt, T. Maeder, L. Sagalowicz, S. Hiboux, S. Scalese, D. Naumovic, R.G. Agostino, N. Xanthopoulos, H.J. Mathieu, L. Patthey, E.L. Bullock, Texture control of $PbTiO_3$ and Pb(Zr,Ti)O_3 thin films with TiO_2 seeding, Journal of Applied Physics 83 (1998) 3835–3841.

[22] J.M. Zeng, M. Zhang, L.W. Wang, C.L. Lin, Influence of lead titanate seed layer on orientation behaviour and ferroelectric characteristics of sol–gel derived PZT thin films, Journal of Physics: Condensed Matter 11 (1999) 1139–1146.

[23] C.J. Kim, B.I. Kim, J. Kim, Effects of $PbTiO_3$ seeding layer on electrical properties of $PbZr_{0.4}Ti_{0.6}O_3$ thin films, Sensors and Actuators A 125 (2006) 353–357.

[24] F.K. Lotgering, Topotactical reactions with ferrimagnetic oxides having hexagonal crystal structures-I, Journal of Inorganic and Nuclear Chemistry 9 (1959) 113–123.

[25] T. Tani, Z.K. Xu, D.A. Payne, Preferred orientations for sol–gel derived PLZT thin layers, Materials Research Society Symposia Proceedings 310 (1993) 269–274.

[26] J. Ricote, R. Poyato, M. Alguero, L. Pardo, M.L. Calazada, Texture development in modified lead titanate thin films obtained by chemistry solution deposition on silicon-based substrate, Journal of the American Ceramic Society 86 (2003) 1571–1577.

[27] X.H. Du, U. Belegundu, K. Uchino, Crystal orientation dependence of piezoelectric properties in lead zirconate titanate: theoretical expectation for thin films, Japanese Journal of Applied Physics 36 (1997) 5580–5587.

[28] D.V. Taylor, D. Damjanovic, Piezoelectric properties of rhombohedral Pb(Zr,Ti)O_3 thin films with (100), (111), and random crystallographic orientation, Applied Physics Letters 76 (2000) 1615–1617.

[29] K.H. Yoon, B.D. Lee, J. Park, Effect of orientation on the dielectric and piezoelectric properties of $0.2Pb(Mg_{1/3}Nb_{2/3})O_3$–$0.8Pb(Zr_{0.5}Ti_{0.5})O_3$ thin films, Applied Physics Letters 79 (2001) 1018–1020.
[30] S.Y. Chen, C.L. Sun, Ferroelectric characteristics of oriented $Pb(Zr_{1-x}Ti_x)O_3$ films, Journal of Applied Physics 90 (2001) 2970–2974.
[31] T.T. Fang, H.L. Hsieh, F.S. Shiau, Effects of pore morphology and grain size on the dielectric properties and tetragonal-cubic phase transition of high-purity barium titanate, Journal of the American Ceramic Society 76 (1993) 1205–1211.
[32] S.H. Yu, Y. Ye, H.T. Huang, L.M. Zhou, Z.Q. Wang, Preparation, structure and properties of $Bi(Mg_{1/2}Ti_{1/2})$–$PbTiO_3$ ceramics and Mn-doping effect, Proceedings of SPIE 6423 (2007) 6423H-1–6423H-4.
[33] R.R.A. Sinha, S. Sharmac, N.K.P. Sinham, Investigation of structural and electrical properties of $(1-x)Bi(Mg_{0.5}Ti_{0.5})O_3$–$xPbTiO_3$ ceramic system, Journal of Alloys and Compounds 486 (2009) 273–277.
[34] L.D. Liu, R.Z. Zuo, Q. Liang, Structure and electrical properties of Mn doped $Bi(Mg1/2Ti1/2)O_3$–$PbTiO_3$ ferroelectric thin films, Applied Surface Science, submitted for publication.